PERIODICA POLYTECHNICA SER. EL. ENG. VOL. 37, NO. 4, PP. 257–272 (1993)

NEW CHALLENGES IN THE VIBRO-ACOUSTICS OF THE INDUCTION MOTOR DRIVES

Peregrin László TIMÁR

Department of Electrical Machines
Technical University of Budapest
H-1521 Budapest, Hungary

Received: April 15, 1993

Introduction

Since Ferraris discovered the idea of the induction motor, this type of motor has been proved as the most reliable, simple, robust and maintenance-free electrical motor. It had, however, one incompleteness, namely the speed can be changed only in complicated ways. The ever-increasing demand for automated drives, the demand for controlled saving in induction motor drives motivated experts to find new solutions. The fast development of the power electronics made the speed variation possible. But, unfortunately, the generous solution, the introduction of the frequency converter is accompanied by several unwanted side effects like increase in audible noise, vibration, additional losses and torque pulsation, etc. This fact is a new challenge for the specialists working in the field of noise and vibration of electrical motors. In this paper, some details will be investigated, how the vibro-acoustic feature of the induction motor changes in variable-speed a.c. drives.

Types of Frequency Converters and the Harmonic Contents of their Output

Most of the modern variable-speed a.c. drives use static converters with intermediate d.c. links and squirrel-cage induction motors. The output voltages and currents of these converters are rich in time harmonics, which detrimentally affects the motor performance.

There are two main types of d.c. link inverters, namely the current source inverters (CSI) and the voltage source inverters (VSI). Both CSIs and VSIs can be classified further into two types: the simple inverters with variable d.c. link voltages (VVSI) and variable d.c. link currents (VCSI), respectively, and inverters with constant d.c. link voltages and constant d.c. link currents, respectively, called pulse width modulated inverters (PWM). Each of these inverters has different output characteristics and different effects on the motor performance.

The electromagnetic noise of an inverter-fed induction motor is strongly influenced by the spectrum of the output voltage/current of the inverter. This statement is valid, irrespective of the type of the inverter, and is only increased by the fact that the magnitude of the induction motor load has a negligible effect only on the magnitude of the time harmonics.

The calculation of the electromagnetic noise and vibration requires the harmonic analysis of the voltage/current supply of the motor in any case. Owing to the numerous individual and often ingenious solutions within the scope of the previously mentioned inverters, this frequency analysis has to be made for each inverter again and again. The expanding in Fourier series is used generally. So, in the following only the general character of the spectrum of the inverter output voltage and current will be presented.

Fig. 1 shows the schematic block diagram of a simple CSI. The amplitude of the output current is changed through the first converter, through the controlled rectifier.

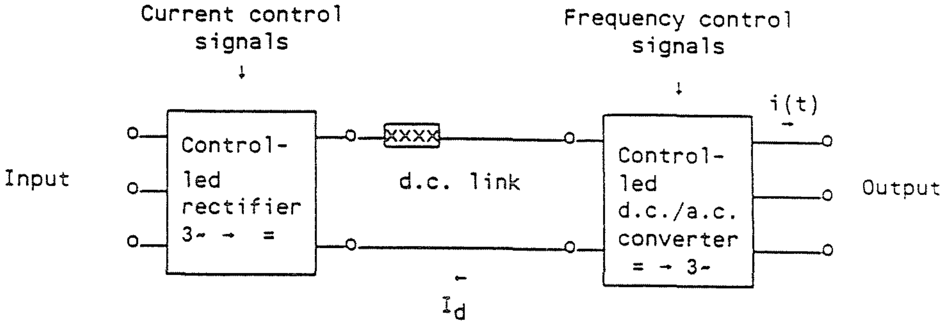

Fig. 1. Block diagram of a simple CSI

The frequency is changed through a d.c./a.c. converter. The machine currents contain besides the fundamental components also time harmonics. The frequency of the harmonic current and, consequently, the angular frequency of the rotating magnetic field, is

$$f_\nu = \nu f_1 \quad \text{and} \quad \omega_\nu = \nu\omega_1 \ , \tag{1}$$

where ν is the order of the time harmonics, $\nu = 6k + 1$ with $k = 0, \pm1, \pm2, \ldots,$ f_1 and ω_1 are the frequency and the angular frequency of the time fundamental wave. The harmonic fields with $k > 0$ rotate in the same direction as the fundamental magnetic field, while those with $k < 0$ rotate in the opposite direction of the fundamental. The magnitude of the time harmonic currents does not depend on the motor parameters in the case of CSIs.

The simple VSI output is a variable amplitude square wave voltage produced by an arrangement shown in *Fig. 2.* It must be mentioned that the switching time in the case of voltage source inverters is very small (much smaller than the switching time at CSI where it has already been neglected) and it may be ignored.

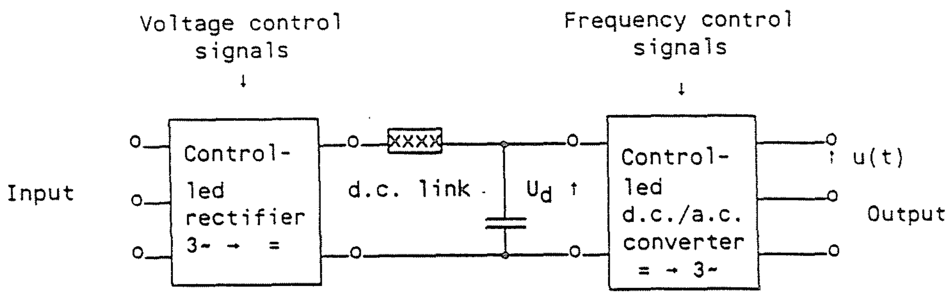

Fig. 2. Block diagram of a simple VSI

The amplitude of the output voltage here is also changed through the controlled rectifier, but the frequency is changed through the d.c./a.c. converter.

The magnitude of the stator current harmonics depends on the machine parameters. The well-known equivalent circuit per phase of an induction motor (see. *Fig. 3*), operated from constant frequency and constant voltage supply is valid also for the fundamental components of voltage and current where the motor is supplied by an inverter. The parameters can be determined from the motor design data or by using experimental methods. For all the time harmonics, R_{Fe} and the main magnetizing field reactance ($\nu\omega_1 L_m$) can be neglected. The slip of the νth time harmonic can be written in the following way:

$$s_\nu = \frac{\nu\omega_1 - \omega}{\nu\omega_1}\ , \quad \text{with} \quad \omega = \omega_1(1/s_1)\ , \quad s_\nu = 1 - \frac{1-s_1}{\nu}\ . \tag{2}$$

Since ν grows rapidly, the harmonic slip s_ν can be approximated by $s_\nu = 1$.

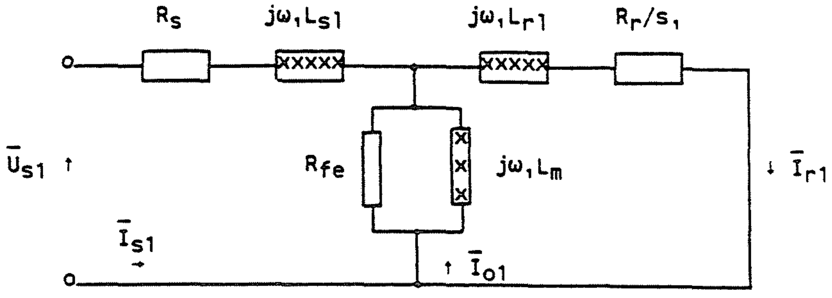

Fig. 3. Equivalent circuit of the induction motor for the fundamental harmonic

For the time harmonics with $|k| > 2$ the calculation error is below 1 per cent at VVI, when a simplified equivalent circuit composed of a pure inductance L_1 might be employed to calculate the harmonic currents (see *Fig. 4*).

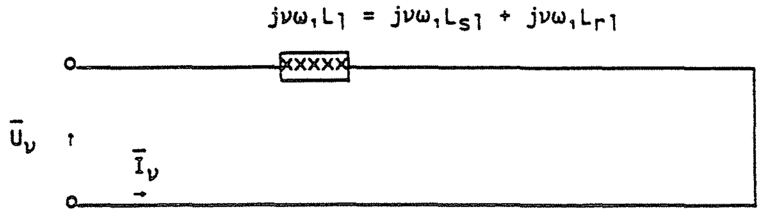

Fig. 4. Equivalent circuit of the induction motor for the high-order time harmonics

The pulse width modulated inverters (PWM) are inverters with constant d.c. link voltages or currents, respectively. *Fig.* 5 illustrates the schematic block diagram of the pulse width modulated voltage source inverter. The control of both the amplitude and frequency of the output voltage is only achieved in the d.c./a.c. converter block. By this method, the ratio of the fundamental a.c. harmonic to the d.c. voltage can be changed. With this decreased ratio, the relative harmonic content of the inverter output voltage will increase.

The harmonic analysis of the PWM inverter output voltage/current is difficult, because there are many variations in the control strategy.

The voltage/current spectrum of the PWM inverters depends on principles subordinated to various optimum criteria. These principles may include – for the given fundamental harmonic voltage/current – e.g. the min-

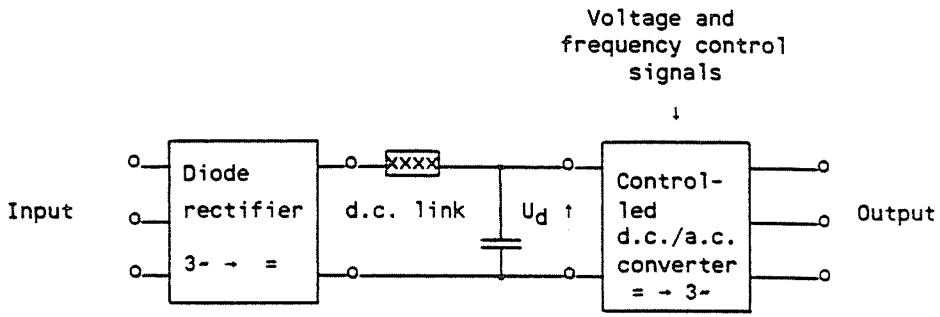

Fig. 5. Block diagram of a PWM VSI

imization of the r.m.s. value of the harmonic content, the elimination of lower-order harmonics, but there are more complicated criteria as well. In each case optimization is achieved by the proper choice of commutation instants of the inverters. The selected optimum criterion, however, has a great impact on the particular quality properties of the drive, e.g. the losses due to the harmonic currents, torque pulsation and speed fluctuation, noise and vibration. While the appropriate loadability requires significant reduction of losses in the full speed range, the decrease of torque pulsation, speed fluctuations and the reduction/elimination of lower-order harmonic pulsations, vibrations and noise are important only at low speeds.

The common character of the output signals in inverters can be demonstrated in the following way:

$$\begin{matrix} u_\nu(t) \\ \text{or} \\ i_\nu(t) \end{matrix} = \sum_\nu \frac{2\sqrt{3}}{\pi} \begin{matrix} U_d \\ \text{or} \\ I_d \end{matrix} \frac{1}{\nu} \cdot f(m)_\nu \cdot \sin(\nu\omega_1 t) = \sum_\nu \begin{matrix} \hat{U}_\nu \\ \text{or} \\ \hat{I}_\nu \end{matrix} \cdot \sin(\nu\omega_1 t) \ , \qquad (3)$$

where U_d and I_d are voltage and current in the d.c. link, $f(m)_\nu$ is the modulation function for the νth harmonic taking the pulse modulation strategy into account. $f(m)_\nu$ has to be determined for each variation of the PWM inverters separately, U_ν and I_ν are the magnitudes of the voltage and current time harmonics. In the case of simple inverters the modulation function equals one.

Field Analysis and Radial Force Waves in Squirrel-Cage Induction Motors

Each time harmonic current induces space harmonics in the air gap of the inverter-fed induction motors due to the slotting of the stator and rotor and due to the eccentricity.

The peripherical distribution of the time harmonic mmf waves corresponds to the distribution of the time fundamental, but the angular velocity is $\nu\omega_1$. The amplitude of the time harmonic mmf waves is inversely proportional to the order of the time harmonics. As the amplitude of the electromagnetic force waves varies with the square of the voltage/current, the space harmonics due to the time harmonic currents must only be taken into account when the amplitude of the time harmonic currents is greater than 70 per cent of that of the time fundamental. If the relation $0.3 < I_\nu/I_1 < 0.7$ exists, then the space harmonics of the current time harmonics, being small in second order, can be neglected. If, however, the time harmonic current is smaller than 30 per cent of the time fundamental, even the space fundamental of the time harmonics can be neglected when calculating the electromagnetic noise/vibration.

When the motor is assumed to be symmetrical electrical and magnetical and the local saturations are neglected, the instantaneous value of the flux density harmonics in the air gap of an inverter-fed induction motor (with slotted stator and rotor) can be written in the following way as the real part of the complex flux density wave:

$$b_{\mu,\nu}(x,t) = \sum_\mu \sum_\nu \hat{B}_{\mu,\nu} \cdot \cos(\mu p x - \nu\omega_1 t) \ , \tag{4}$$

where p is the pole pair number of the motor, x is the space coordinate along the centre line of the air gap, μ is the order of the stator space harmonics ($\mu = 2mg + 1$ with $g = 0, \pm1, \pm2, \dots$).

It is worth dividing this twofold Fourier series into two groups. Firstly, because of their importance, one can take the space fundamental ($\mu = 1$) of all the time harmonic currents (see in *Fig.* 6 marked with x). The flux density has the following expression:

$$b_{\mu=1,\nu}(x,t) = \sum_\nu \hat{B}_{\mu=1,\nu} \cdot \cos(px - \nu\omega_1 t) \tag{5}$$

The amplitude of these harmonics can be written as:

$$\hat{B}_{\mu=1,\nu} = \frac{m\hat{I}_\nu N_1 K_p}{p\pi} \cdot \frac{F_{m,\text{tot}}}{F_{m,\text{air gap}}} \cdot \frac{\mu_0}{\delta_g k_{c1} k_{c2}} \ , \tag{6}$$

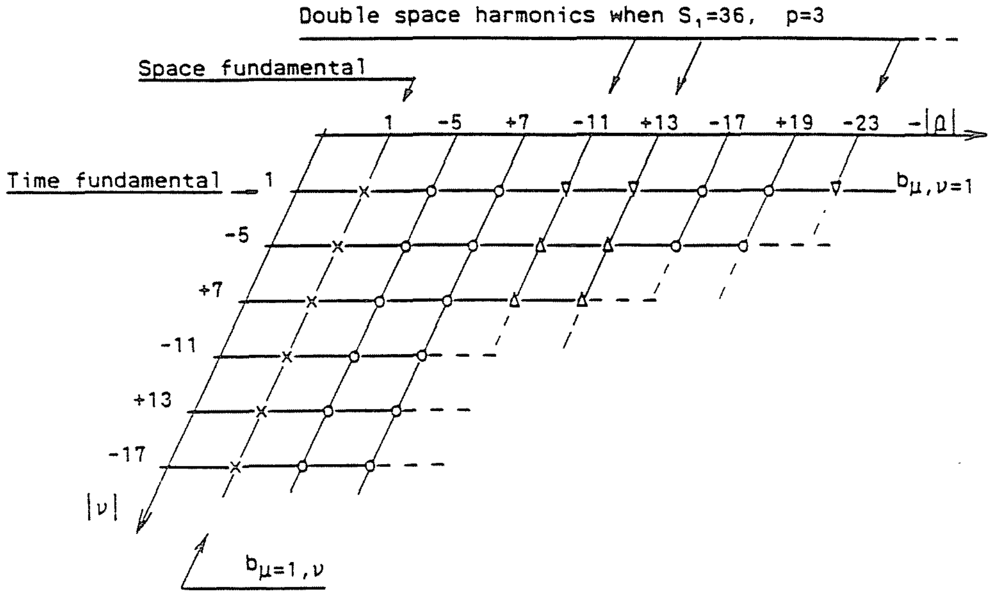

Fig. 6. The $b_{\mu,\nu}$ field when $\mu = 2mg + 1 = 6g + 1$ (if $m = 3$), $\mu_{s1} = 1 + gS_1/p$, $g = 0, \pm 1, \pm 2, \dots$, $\nu = 6k + 1$, $k = 0, \pm 1, \pm 2, \dots$

where $\hat{I}_\nu$ is the peak value of the νth time harmonic stator current, m is the number of phase, N_1 is the number of turns in one stator phase winding, K_p is the resultant winding factor for the space fundamental harmonic on the stator, $F_{m,\text{tot}}$ is the total mmf summed up in the magnetic circuit of the motor, $F_{m,\text{air gap}}$ is the mmf on the air gap, δ_g is the radial air gap dimension between the cylindrical surfaces of the stator and rotor limiting the air gap and k_{c1} and k_{c2} are the Carter factors for the stator and rotor, respectively.

The flux density space harmonics in the air gap are forming the second group ($\mu \neq 1$) These space harmonics are caused by slotting, and include the so-called winding and slot harmonics. Here one has to take into consideration the space harmonics of the time fundamental mmf wave and the space harmonics of the mmf time harmonics (taking the aforesaid restricting remarks into account). The flux density space harmonics can be expressed as:

$$b_{\mu\neq 1,\nu}(x,t) = \sum_{\mu}\sum_{\nu} \hat{B}_{\mu\neq 1,\nu} \cdot \cos(\mu p x - \nu\omega_1 t) \ . \tag{7}$$

The amplitude $\hat{B}_{\mu\neq 1,\nu}$ can be written generally in the following way:

$$\hat{B}_{\mu=1,\nu} = \frac{m\hat{I}_\nu N_1 K_\mu}{\mu p \pi} \cdot \frac{F_{m,\text{tot}}}{F_{m,\text{air gap}}} \cdot \frac{\mu_0}{\delta_g k_{c1} k_{c2}} \ , \tag{8}$$

where K_μ is the resultant winding factor for the μth space harmonic on the stator.

When the winding and slot harmonics are existing simultaneously having the same order ($\mu = \mu_{sl}$) with $\mu = 2mg+1$, $\mu_{s1} = 1+g'S_1/p$ (where g and g' are different values of g), then the amplitude of the flux density space harmonic is the resultant of the two amplitudes. Computing this resultant amplitude, one has to distinguish between the space harmonics of the time fundamental and the space harmonics of the time harmonics. If $\nu = 1$, and $2mg = g'S_1/p$ (see *Fig. 6* marked with ∇), then the amplitude can be approximated by the following expression:

$$\hat{B}_{\mu\neq 1,\nu=1} = \frac{mN_1}{p\pi} \cdot \frac{\mu_0}{\delta_g k_{c1} k_{c2}} \cdot \sqrt{A^2 + B^2 + 2AB\cos\phi_1}\ , \tag{9}$$

where

$$A = \frac{\hat{I}_1 K_\mu}{\mu} \cdot \frac{F_{m,\mathrm{tot}}}{F_{m,\mathrm{air\ gap}}}$$

and

$$B = -(-1)g' \cdot \frac{2\hat{I}_m K_p}{g'\pi} \cdot k_{c1} \cdot \sin \cdot \left(g'\pi \frac{k_{c1} - 1}{k_{c1}}\right)\ .$$

where $\hat{I}_1$ is the fundamental harmonic of the stator current, ϕ_1 is the phase angle belonging to $\hat{I}_1$ and $\hat{I}_m$ is the peak value of the magnetizing current (can be approximated by the no-load stator current).

For the time harmonics ($\nu \neq 1$), when $2mg = g'S_1/p$ (see *Fig. 6* marked with $\triangle$) the amplitude of the space harmonics can be approximated by the following expression:

$$\hat{B}_{\mu\neq 1,\nu\neq 1} = \frac{mN_1}{p\pi} \cdot \frac{\mu_0}{\delta_g k_{c1} k_{c2}} \cdot \left[A\frac{I_\nu}{I_1} + B\frac{I_\nu}{I_m}\right]\ . \tag{10}$$

The voltages induced in the rotor winding by the $b_{\mu\neq 1,\nu}$ stator flux density harmonics give rise to the rotor mmf waves which cause the rotor flux density space harmonics. (That means the so-called rotor rest fields caused by the stator space harmonics will be neglected.) The rotor flux density space harmonics can be written in the following way:

$$b_{\lambda,\nu}(x,t) = \sum_\lambda \sum_\nu \hat{B}_{\lambda,\nu} \cdot \cos(\lambda p x - \omega_{\lambda,\nu} t)\ , \tag{11}$$

where λ is the order of the rotor flux density space harmonics (in the case of squirrel-cage rotor $\lambda = 1 + gS_2/p$), $\omega_{\lambda,\nu}$ is the angular frequency of the rotor space harmonics.

$$\omega_{\lambda,\nu} = \omega_1[\nu + gS_2(1 - s_1)/p]$$

and the amplitude can be approximated as follows:

$$\hat{B}_{\lambda,\nu} = \frac{mN_1}{p\pi} \cdot \frac{\mu_0}{\delta_g k_{c1} k_{c2}} \cdot \left[\frac{\hat{I}_\nu K_\lambda}{\lambda} - (-1)G \cdot \frac{2\hat{I}_\nu K_p}{g\pi} \cdot k_{c2} \cdot \sin(g\pi \frac{k_{c2}-1}{k_{c2}}) \right] . \tag{12}$$

If there is the time fundamental wave ($\nu = 1$), then

$$\hat{B}_{\lambda,\nu=1} = \frac{mN_1}{p\pi} \cdot \frac{\mu_0}{\delta_g k_{c1} k_{c2}} \cdot \sqrt{C^2 + D^2} , \tag{13}$$

where $C + \frac{\hat{I}_1 \cos\phi_1 K_\lambda}{\lambda}$ and $D = \frac{2\hat{I}_m K_p}{g\pi} \cdot k_{c2} \cdot \sin(g\pi \frac{k_{c2}-1}{k_{c2}})$.

The flux density space harmonics of the rotor due to the rotor eccentricity are found as:

$$b_{\lambda e,\nu}(x,t) = \sum_{\lambda_e} \sum_{\nu} \hat{B}_{\lambda e,\nu} \cdot \cos\left[(\lambda p \pm 1)x - \omega_{\lambda e,\nu} t)\right] , \tag{14}$$

where $\omega_{\lambda e,\nu}$ is the angular frequency of the rotor flux density space harmonics due to the rotor eccentricity, $\omega_{\lambda e,\nu} = \omega_1[\nu + (gS_2 \pm 1)(1 - s_1)/p]$ and the amplitude can be written in the following way:

$$\hat{B}_{\lambda e,\nu} = -(-1)g \cdot \frac{m_\nu \hat{I}_1 N_p K_\lambda K}{\lambda p\pi} \cdot \frac{\mu_0 e}{(\delta_g k_{c_1} k_{c2})^2} , \tag{15}$$

where e is the eccentricity of the rotor.

The resultant air gap flux density can be expressed by the following groups of harmonics:

$$b = b_{\mu=1,\nu} + b_{\mu\neq1,\nu} + b_{\lambda,\nu} + b_{\lambda e,\nu} . \tag{16}$$

Radial Electromagnetic Forces in Inverter-Fed Induction Motors

The radial force acting per unit surface area (the radial tensile stress) can be calculated according to Maxwell's law:

$$p(x,t) = b^2(x,t)/2\mu_0 , \tag{17}$$

After substituting all flux density components and calculating the radial tensile stress components one can get an infinite number of radial force waves. Any component of the force wave, acting over a unit area, may be written in the following form:

$$p(x,t)_r = P_r \cos(rx - \omega_r \hat{t}) \ , \tag{18}$$

where r is the mode number of the force wave, ω_r is the angular frequency and P_r is the amplitude of the rth force wave.

At the squares of the flux density waves, the mode number and the frequency are equal to zero or double the order and frequency of the flux density wave, the amplitude is the square of the flux density wave amplitude divided by $2\mu_0$. In the case of mixed products of the constituting flux density waves, the mode number and the frequency of the force wave can be calculated as the sum or the difference of the orders or frequencies of the constituting flux density waves. The amplitude of the force wave is the product of the flux density wave amplitudes divided by $2\mu_0$. In order to get an easy survey, the mode numbers and frequencies of all the force wave groups are listed in *Table 1.*

Table 1

The mode numbers and frequencies of the electromagnetic force wave components

Constituting flux density waves	Mode number (r)	Frequency (f_r)
$b^2_{\mu=1,\nu}$	0 or $2p$	$\underline{\underline{2}}$ or $2\nu f_1$
$b^2_{\mu\neq1,\nu}$	0 or $\underline{4mgp+2p}$	$\underline{\underline{2}}$ or $2\nu f_1$
$b^2_{\lambda,\nu}$	0 or $\underline{2gS_2+2p}$	$\underline{\underline{0}}$ or $2f_1[\nu + gS_2(1-s_1)/p]$
$b^2_{\lambda e,\nu}$	0 or $\underline{2gS_2+2p\pm2}$	$\underline{\underline{0}}$ or $2f_1[\nu + (gS_2 \pm 1)(1-s_1)/p]$
$2b_{\mu=1,\nu}b_{\mu'\neq1,\nu'}$	0 or $2p$	$f_1[6(k\pm k') + 0 \text{ or } 2]$
$2b_{\mu\neq1,\nu}b_{\nu'\neq1,\nu'}$	$\underline{2mp(g\pm g') + 0 \text{ or } 2p}$	$f_1[6(k\pm k') + 0 \text{ or } 2]$
$2b_{\lambda,\nu}b_{\lambda,'\nu'}$	$\underline{S_2(g\pm g') + 0 \text{ or } 2p}$	$f_{\lambda,\nu} \pm f_{\lambda,'\nu'}$
$2b_{\lambda e,\nu}b_{\lambda e,'\nu'}$	$\underline{S_2(g\pm g') + (0 \text{ or } 2p)}$ $\underline{+(0 \text{ or } \pm 2)}$	$f_{\lambda e,\nu} \pm f_{\lambda e,'\nu'}$
$2b_{\mu=1,\nu}b_{\mu\neq1,\nu}$	$\underline{p(2mg + (0 \text{ or } 2)}$	$f_1[6(k\pm k') + 0 \text{ or } 2]$
$2b_{\mu=1,\nu}b_{\lambda,\nu}$	$\underline{gS_2 + 0 \text{ or } 2p}$	$f_1[gS_2(1-s_1)/p + 0 \text{ or } 2\nu]$
$2b_{\mu=1,\nu}b_{\lambda e,\nu}$	$\underline{gS_2 + 0 \text{ or } 2p \pm 1}$	$f_1[gS_2 \pm 1(1-s_1)/p + 0 \text{ or } 2\nu]$
$2b_{\mu\neq1,\nu}b_{\lambda,\nu}$	$gS_2 \pm 2mg'p + 0 \text{ or } 2p$	$f_1[gS_2(1-s_1)/p + 0 \text{ or } 2\nu]$
$2b_{\mu\neq1,\nu}b_{\lambda e,\nu}$	$gS_2 \pm 2mg'p + 0 \text{ or } (2p\pm1)$	$f_1[gS_2 \pm 1(1-s_1)/p + 0 \text{ or } 2\nu]$
$2b_{\lambda,\nu}b_{\lambda e,\nu}$	$\underline{0 \text{ or } (2gS_2 + 2p \pm 1)}$	$f_1[\frac{S_2(1-s_1)(g\pm g')\pm(1-s_1)}{p} + 0 \text{ or } 2\nu]$

The positive sign of the force mode number means that the force wave component rotates in the same direction as the rotor does, while the negative sign means that the force wave component rotates in the opposite direction.

Based on theoretical considerations and practical experience, the force waves classified dangerous in terms of vibration or noise can be selected on the basis of their mode numbers and frequencies. The low and medium power induction motors have proved to be extremely rigid to force waves with mode numbers over 6. Therefore, one can neglect the analysis of force waves having mode numbers over six. At high-power induction motors this mode number limit can go up to 8. By experience, the frequency range of 200 Hz ... 5 000 Hz must be considered as dangerous for noise, and the frequency range of 10 Hz ... 2 000 Hz for vibration.

A strong selection can be made in the infinite large set of the force wave components based on these mode number and frequency stipulations. It is marked with a single underlining when a force component can be neglected due to the mode number stipulation (the mode number is too high) and with a double underlining when a force wave component can be neglected due to the frequency stipulation (the frequency is out of the given frequency range). So it can be stated that the following terms are dangerous as to noise/vibration generation:

$$
\begin{aligned}
&\sum_{\nu}[\hat{B}^2_{\mu=1,\nu}/2\mu_0] - \cos(2px - 2\nu\omega_1 t)\ ,\\
&\sum_{\nu}\sum_{\nu'}[\hat{B}_{\mu=1,\nu}\hat{B}_{\mu=1,\nu'}/\mu_0] - \cos[6(k-k')\omega_1 t]\ ,\\
&\sum_{\nu}\sum_{\nu'}[\hat{B}_{\mu=1,\nu}\hat{B}_{\mu=1,\nu'}/\mu_0] - \cos{-2px} - [6(k+k')+2]\omega_1 t-\ ,\\
&\sum_{\mu}\sum_{\lambda}\sum_{\nu}[\hat{B}_{\mu\neq1,\nu}\hat{B}_{\lambda,\nu}/\mu_0] - \cos{-[gS_2 - 2mg'p]x-}\\
&\quad - [gS_2(1-s_1)/p]\omega_1 t-\ ,\\
&\sum_{\mu}\sum_{\lambda}\sum_{\nu}[\hat{B}_{\mu\neq1,\nu}\hat{B}_{\lambda,\nu}/\mu_0] - \cos{-[gS_2 + 2mg'p + 2p]x}\\
&\quad - [gS_2(1-s_1)/p + 2\nu]\omega_1 t-\ ,\\
&\sum_{\mu}\sum_{\lambda e}\sum_{\nu}[\hat{B}_{\mu\neq1,\nu}\hat{B}_{\lambda e,\nu}/\mu_0] - \cos{-[gS_2 - 2mg'p - 1]x}\\
&\quad - [(gS_2-1)(1-s_1)/p]\omega_1 t-\ ,\\
&\sum_{\mu}\sum_{\lambda e}\sum_{\nu}[\hat{B}_{\mu\neq1,\nu}\hat{B}_{\lambda e,\nu}/\mu_0] - \cos{-[gS_2 + 2mg'p + 2p]x}\\
&\quad - [(gS_2-1)(1-s_1)/p + 2\nu]\omega_1 t-\ .
\end{aligned}
\tag{19}
$$

The triple summing up suggests a frighteningly long calculation process. However, in practice and taking the magnitude stipulation related to the time harmonics (presented previously) into consideration the number of the time harmonics and their space harmonics to be considered is limited.

After analyzing the mode numbers of the force waves collected, one can conclude that the time harmonic currents due to the inverters do not generate new mode numbers compared to the work of the motor supplied purely sinusoidally. But there are many new force wave components with different new frequencies. In the case of sinusoidal feeding the square of the fundamental wave has a frequency equal to $2f_1$, so it is dangerous in terms of vibration only. Now, the frequency of the $b^2_{\mu=1,\nu}$ component is $2\nu f_1$ already inside in the frequency range of the audible noise. The $b_{\mu=1,\nu}b_{\mu=1,\nu'}$ mixed products, unknown in the case of induction motors fed purely sinusoidally, are dangerous both in terms of vibration and noise. The b_μ b_λ and b_μ $b_{\lambda e}$ mixed products are traditionally dangerous in terms of noise and vibration. However, in the case of inverter feeding they have new force components with new frequencies characterized by the new member ν in the expression of the frequencies.

Vibration of Electromagnetic Origin

Previously, the radial force waves acting on the rotating electrical machine have been determined and found to be waves of different mode numbers and different distribution in the air gap round the periphery. These waves propagate with different angular velocities round the rotor in the same or opposite sense as the rotor rotates, acting both on the stator and the rotor. With the exception of the bending force wave of mode number $n = 1$, all exciting forces result in a more significant deformation of the stator. For $n = 1$ the rotor seems to be more flexible. Bending forces of mode number $n = 1$ present the greatest problem in high-power rotating machines with a flexible rotor and large bearing span. (A rotor is called flexible if its first critical speed is below or just above the rotational speed of the rotor.) It may be mentioned that in the literature there are published some approximative formulas for the determination of the first critical rotational frequency of the most common low and medium power machines.

Any force wave of frequency f_n and mode number n gives rise to a set of vibrations of order j and frequency f_n in the rotating electrical machine. The magnitudes of vibration components depend on the geometric dimensions of the machine, the magnitude of the exciting force, the difference between the frequency f_n of the exciting force and the resonance frequencies $f_{\text{res},j}$ of the machine and on the damping conditions inside the machine. If the frequency f_n is close to or equal to any of the resonance frequencies of the machine, then resonance occurs, which results in dangerous vibrations and a substantial increase in noise.

The rms value of the vibrational velocity produced by a force wave with the amplitude P_n, frequency f_n and mode number n is found as

$$\nu_{fn} = \sqrt{2}\pi f_n \sum_j H_j \hat{P}_n \ , \tag{20}$$

where H_j is the system function of the electrical machine as a vibrating mechanical system.

The system function H_j represents the relationship between the force acting upon the system and the vibration deformation excited by it. It is split into two components, as commonly found in the literature. One of them, $H_{j,\text{static}}$, contains the geometrical dimensions of the machine, the quality of the material and the mode number j. This component provides the deformation for the case where the mode number of the exciting force n equals the mode number of deformations j and the frequency is $f_n = 0$, i.e. the deforming force will not vary in time. The second component $H_{j,\text{dynamic}}$ depends on the distance between f_n and the mechanical resonance frequency $f_{\text{res},j}$ (characteristic of the vibration mode number j), and on the internal damping conditions. This $H_{j,\text{dynamic}}$ component is sometimes referred to as the magnification factor and has the form:

$$H_{jm} = \frac{1}{\sqrt{[1-(f_n/f_{j,\text{res}})^2]^2 + 4D^2(f_n/f_{j,\text{res}})^2}} \ , \tag{21}$$

where $f_{j,\text{res}}$ is the resonance frequency of the machine for the vibration mode j, and D is the inner Lehr's damping factor. The computation of the two components of the system function H_j can be found in relevant literature.

It is worth noting that the vibrating capability of the machine improves with increasing sizes and that the mechanical resonance frequencies become lower, which makes the resonance frequencies of higher mode number appear within the audible range.

The main source of the damping D is the friction on the contacting surfaces of the winding and the laminated core. The theoretical determination of damping is extremely complex, therefore it is often derived experimentally. For induction motors the value of D is usually approximately 0.01-0.03.

The coincidence of the frequency of the exciting force and the mechanical resonance frequency of the machine results in resonance. This may occur in static operation at constant speed or may even occur in transient operation. The equation of the frequency of the electromagnetic exciting forces, in the induction motor, for instance, shows that the value of f_n changes linearly with the speed. Therefore, resonance may occur in the acceleration period in cases where the mechanical natural frequency of the machine in steady-state operation is much lower than the frequency of the exciting force. In other words, the smoothly running machine might 'roar up 'during the acceleration period. This transient resonance may show up under other types of transient operating conditions, like reversing, or in the generator braking mode of multi-speed motors. This problem gets more importance from day to day and, therefore, it will be necessary to investigate it more thoroughly in the future.

Sound of Electromagnetic Origin

The sound power with the frequency of f_n, emitted by the electrical machine into the environment, can be calculated with *Eq.*(22):

$$P_{fn} = \rho c \sigma \nu_{fn}^2 S_{\mathrm{rad}} \ , \tag{22}$$

where ρ is the density of medium, c is the speed of sound in the medium (the value of ρc for room temperature is 415 $\mathrm{Ns/m^3}$), σ is the radiation factor, ν_{fn} is the rms value of the mechanical vibration velocity measured on the surface of the machine, f_n is the frequency of the vibration and S_{rad} is the machine surface taking part in the radiation. It is quite difficult to determine the value of S_{rad} in the case of complex-shaped electrical machines. According to experience, the role of ribs in emitting sound is not significant. Thus, the S_{rad} can be substituted by the cylindrical or rectangular surface enveloping the machine.

The electric machines have complex shapes and their sound radiation factor is, therefore, examined on simplified models. The modelling of the electrical machine with an infinitely long cylinder gives only a satisfactory result for the central section of a machine with a large l/D ratio (where l is the length of the assembled machine, and D is the outer diameter of the cylindrical machine). The endeffect due to the finite length of the cylinder can be neglected only in the case of a very long machine. If the surface of the machine is made of large planes (in the case of the rectangular shape housings used nowadays at the large powered machines), it is sufficient to assume the machine as a plane-radiator. In the most common case, at small and medium-sized electrical machines the sphere model seems to be suitable.

The force waves lead to a deformation going around the machine having an outer diameter D. This is the diameter of the sphere in the case of a spherical radiator and the diameter of the cylinder in the case of a cylindrical radiator. D seems to be the characteristic dimension of the machine from point of view of the sound radiation (the use of the diameter is preferred in praxis instead of the radius).

The radiation factor is usually described with a complicated formula. For instance, in the case of the ideal spherical radiator of mode number n it is:

$$\sigma_n = \mathrm{Re}\left\{ \frac{jkD}{2} \frac{\sum_{i=1}^{n-1} \frac{(n+i)!}{(n-i)!}\frac{n!}{i!}(jkD)^{n-i}}{\sum_{i=1}^{n-1} \frac{(n+i)!}{(n-i)!}\frac{n!}{i!}(jkD)^{n-i}(1+0.5jkD+i)} \right\}, \qquad (23)$$

where $k = 2\pi f_n/c$ is the wave number, i is an integer.

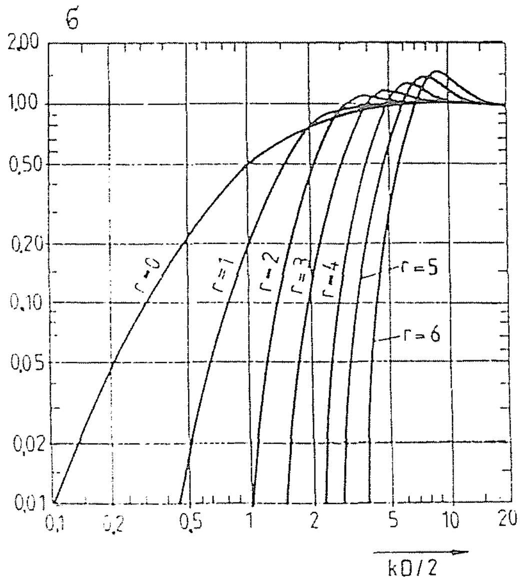

Fig. 7.

Eq. (23) shows that the σ radiation factor depends on the dimensions of the machine, the mode number and the frequency. The application of the formula for the radiation factor is difficult. It is usually used in the form of a group of curves (see *Fig. 7*).

The radiation factor given in *Eq.* (23) can be approximated up to $n = 5$ with a simple power function presented in *Eq.* (24)

$$\sigma_n = \frac{K^{2n+2}}{A + K^{2n+2}} \cdot [B \cdot 10^{-3}(K-20)^2 + 1] , \tag{24}$$

where $K = kD/2$ and A as well as B are constants with the following values:

$n =$	0	1	2	3	4	5
$A =$	1	4	10^2	$5 \cdot 10^3$	$5 \cdot 10^5$	10^8
$B =$	0	0	0.4	1.11	1.51	2.11

If the frequency as well as the size of the machine are large, the electrical machine will act as a plane radiator, then $\sigma = 1$. It can be stated irrespective of the type of sound-radiating model that machines of small dimensions are bad radiators of sound, while machines of large dimensions radiate sound well.

If many independent components of vibration produce the noise of the electrical machine, the resultant sound power of the electrical machine will be the sum of the sound powers of the components.

References

1. HELLER, B. – HAMATA, V. (1977): Harmonic Field Effects in Induction Machines. Elsevier, Amsterdam.
2. TIMÁR, P. L. (1975): Die Auswirkung der Stromrichtergespeisung auf das Geräuschverhalten des Asynchronmotors mit Schleifringläufer. *I. Symposion regional contre le bruit.* Varna.
3. TIMÁR, P. L. (1976): Noise Problems of the Asynchronous Machine Fed by an Inverter. *ICEM'76.*
4. TIMÁR, P. L. (1985): Theory of the Vibration and Noise of Asynchronous Machines and the Experimental Investigation. Thesis for the D.Sc. degree. Budapest.
5. ISO 1680/1,2. Test Code for the Measurement of Airborne Noise Emitted by Rotating Electrical Machinery.
6. TIMÁR, P. L. (1989): Noise and Vibration of Electrical Machines. Elsevier, Amsterdam, New-York.